Defense Technical Information Center Compilation Part Notice

ADP012657

TITLE: Strategies for Direct Monolithic Integration of AlxGa[1-x]As/InxGa[1-x]As LEDS and Lasers On Ge/GeSi/Si Substrates Via Relaxed Graded GexSi[1-x] Buffer Layers

DISTRIBUTION: Approved for public release, distribution unlimited

This paper is part of the following report:

TITLE: Progress in Semiconductor Materials for Optoelectronic Applications Symposium held in Boston, Massachusetts on November 26-29, 2001.

To order the complete compilation report, use: ADA405047

The following component part numbers comprise the compilation report:
ADP012585 thru ADP012685

Mat. Res. Soc. Symp. Proc. Vol. 692 © 2002 Materials Research Society

Strategies For Direct Monolithic Integration of $Al_xGa_{(1-x)}As/In_xGa_{(1-x)}As$ LEDS and Lasers On Ge/GeSi/Si Substrates Via Relaxed Graded $Ge_xSi_{(1-x)}$ Buffer Layers

Michael E. Groenert, Christopher W. Leitz, Arthur J. Pitera, Vicky K. Yang, Harry Lee*, Rajeev J. Ram*, and Eugene A. Fitzgerald

Department of Materials Science and Engineering, MIT, Cambridge, MA 02139, U.S.A.
*Department of Electrical Engineering and Computer Science, MIT, Cambridge, MA 02139, U.S.A.

ABSTRACT

$Al_xGa_{(1-x)}As/GaAs$ quantum well lasers have been demonstrated via organometallic chemical vapor deposition (OMCVD) on relaxed graded $Ge/Ge_xSi_{(1-x)}$ virtual substrates on Si. Despite un-optimized laser structures with high series resistance and large threshold current densities, surface threading dislocation densities as low as $2x10^6$ cm^{-2} enabled cw room-temperature lasing at a wavelength of 858nm. The laser structures are oxide-stripe gain-guided devices with differential quantum efficiencies of 0.16 and threshold current densities of $1550A/cm^2$. Identical devices grown on commercial GaAs substrates showed differential quantum efficiencies of 0.14 and threshold current densities of $1700A/cm^2$. This comparative data agrees with our previous measurements of near-bulk minority carrier lifetimes in GaAs grown on Ge/GeSi/Si substrates. A number of GaAs/Ge/Si integration issues including thermal expansion mismatch and Ge autodoping behavior in GaAs were overcome.

INTRODUCTION

Semiconductor lasers remain a primary goal for GaAs on Si integration due to their proven usefulness in a wide variety of optoelectronic applications, but they also remain the most difficult devices to demonstrate successfully. As high-power minority carrier devices, semiconductor lasers are very sensitive to epitaxial material quality and crystal defect density. Early attempts to grow reliable GaAs lasers directly on Si using a wide variety of epitaxial techniques were unsuccessful [1]. The 4.1% lattice mismatch between GaAs and Si leads to unacceptably high densities of threading dislocation defects ($> 10^8$ cm^{-2}) in the active regions of lasers grown directly on Si, resulting in very short device lifetimes. More recently, alternative techniques involving wafer bonding [2], epitaxial lateral overgrowth [3] and migration-enhanced epitaxy [4] were investigated for integration applications. While bonding in particular has attracted much interest, this technique is inherently cost-limited as device density increases, and faces continued difficulties with contact resistance at the bond interface.

Continuing work in our group has demonstrated an alternative approach to successful monolithic GaAs on Si integration making use of relaxed graded Ge/GeSi buffer layers [5]. Ting [6] has demonstrated high-quality diode structures on Ge/GeSi buffers on Si and has shown how past difficulties with anti-phase boundary (APB) formation at the GaAs/Ge interface can be avoided with high-temperature initiation on deliberately offcut substrates. Surface threading dislocation densities in these samples have been measured at 2×10^6 cm^{-2} using defect selective etching and plan-view transmission electron microscopy (TEM). Minority carrier lifetime measurements for GaAs films grown on GeSi/Ge buffers [7] have shown lifetimes comparable to

bulk GaAs, indicating that the mean dislocation spacing has approached the minority carrier diffusion length in this optimized material.

The thermal expansion coefficient of Si is significantly smaller than GaAs. Consequently, growth of GaAs on Si substrates by high-temperature CVD leads to trapped tensile strain in GaAs device layers on Ge/GeSi/Si. Efforts have been taken to reduce this tensile strain by introducing deliberate compressive strain in the Ge/GeSi buffer layers [5]. This compressive strain yields cubic Ge layers on Si after cooldown at room temperature, but at the cost of increased compressive strain and imperfect GaAs/Ge lattice matching at the growth temperature. Compressive strain in the Ge buffer will limit the critical thickness for strained $In_xGa_{(1-x)}As$ quantum wells in GaAs grown above it.

GaAs grown on Ge can introduce complications for device integration due to autodoping effects from amphoteric Ge moving into the GaAs above it. This Ge can act to compensate intentional dopants in GaAs device layers and increase free-carrier absorption in laser active regions. Work by Srinivasan [8] and others [9],[10] has shown that autodoping can occur via transport in the vapor phase during film growth, and that this gas-phase reaction depends strongly on reactor pressure and on the temperature and time of pregrowth annealing.

In the present study, GaAs/AlGaAs/InGaAs laser structures were grown on relaxed graded Ge/GeSi graded buffers on Si substrates and compared to identical lasers on commercial GaAs substrates. The initial structures and growth recipes were then modified to account for thermal expansion effects and Ge autodoping in the devices grown on Ge/GeSi/Si.

EXPERIMENTAL DETAILS

All laser structures were grown in an atmospheric organometallic chemical vapor deposition (OMCVD) reactor operating at 750 °C. Commercial (100) n+ GaAs substrates offcut 2° towards [110] were used as controls. For growth on Si, relaxed Ge on graded $Ge_xSi_{(1-x)}$ buffers on (100) Si offcut 6° towards the [110] were used. The details of the Ge/GeSi buffer growth process and its optimization for GaAs growth has been reported elsewhere [5].

The laser structures grown for these experiments were AlGaAs/GaAs/InGaAs graded index separate confinement heterostructure (GRINSCH) quantum-well devices. The structure is shown in Figure 1. The growths began with a 500nm GaAs buffer ($n = 6 \times 10^{18}$ cm^{-3}) followed by a 1.1 μm $Al_{0.6}Ga_{0.4}As$ cladding layer ($n = 4 \times 10^{18}$ cm^{-3}). After this a symmetric graded $Al_xGa_{(1-x)}As$ structure ($x = 0.6$ to 0.2) centered around an 8 nm $In_{0.2}Ga_{0.8}As$ quantum well was

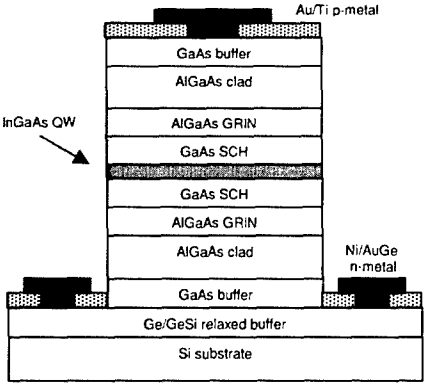

Figure 1: Schematic of laser structure used for this experiment. Devices with 10nm GaAs QWs and $Al_{0.2}Ga_{0.8}As$ SCHs were also grown to avoid misfit dislocations in the quantum wells.

grown without doping. This structure was capped with another 1.1 μm $Al_{0.6}Ga_{0.4}As$ cladding layer ($p = 2 \times 10^{17}$ cm^{-3}) and a highly doped 50nm GaAs contact layer ($p = 1 \times 10^{19}$ cm^{-3}). Film thicknesses were confirmed with TEM, and dopant concentrations were measured using secondary ion mass spectroscopy (SIMS).

Oxide-stripe gain-guided devices were fabricated from these structures with 5 μm stripe-widths. To reduce series resistance through the substrate, n-side contact stripes were etched through the GaAs layers to the Ge buffer layer, defining wide (100 μm) ridge waveguides. Devices were then thinned and cleaved into bars of varying lengths.

RESULTS AND DISCUSSION

$In_{0.2}Ga_{0.8}As$ quantum well lasers grown on GaAs substrates operated cw at room temperature and demonstrated a threshold current density of 1370 A/cm^2 and a differential quantum efficiency of 0.30 at a wavelength of 1005 nm. Identical devices grown on Ge/GeSi/Si substrates did not lase and showed a subthreshold differential quantum efficiency of 7.1×10^{-6}. Cross-sectional TEM of similar devices on Ge/GeSi/Si substrates showed misfit dislocations in the quantum well, indicating that the critical thickness for $In_{0.2}Ga_{0.8}As$ in these samples was less than 8 nm. As mentioned above, the reduced critical thickness for compressive InGaAs on a Ge/GeSi/Si substrate is likely due to the increased compressive strain in the Ge/GeSi buffer layer at the growth temperature.

SIMS scans of similar structures on Ge/GeSi/Si substrates in Figure 2a show uniform Ge contamination in all layers of the GaAs device at concentrations of 1×10^{18} cm^{-3} or higher. The flat Ge doping profile throughout the device structure with a small peak in the low-growth-rate quantum well region confirms the dominance of vapor-phase transport from external sources over other autodoping mechanisms such as solid-state diffusion, which would be expected to show a decreasing Ge concentration with device thickness. The high pressures and temperatures present in the OMCVD growth chamber, coupled with a 5-minute pregrowth anneal step at 700 °C provided ample opportunity for Ge substrate evolution into the vapor phase and subsequent deposition in the GaAs/AlGaAs/InGaAs device layers.

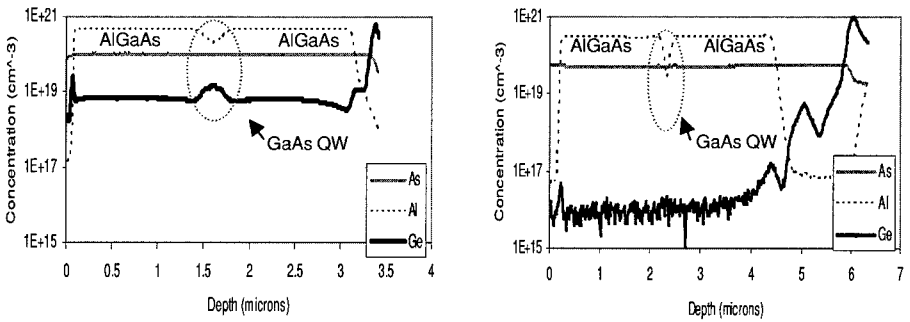

Figure 2: SIMS data showing (a.) Ge contamination in device layers and (b.) reduced contamination with the improved recipe to remove Ge vapor sources in the reactor

To avoid the difficulties with compressive strain introduced by the Ge/GeSi buffer layers, identical laser structures were grown substituting a 10nm GaAs quantum well for the 8nm InGaAs quantum well. The GaAs quantum well removes the problem of strain-induced misfit dislocations in the quantum well at the cost of reduced electrical and optical confinement and less resistance to dark-line defects [11].

To reduce the high Ge autodoping in the device layers, a series of experiments was run to pinpoint the chief sources of Ge in the growth sequence. Four steps were taken to remove potential sources for gas-phase Ge evolution: 1.) cleaning the reactor tube, 2.) changing the graphite susceptor the sample rests on during growth, 3.) capping the front Ge/GeSi surface with GaAs, and 4.) polishing the wafer backside to remove Ge underneath the device. Reducing the reactor pressure or growth temperature may reduce autodoping; but this is not possible with the available CVD reactor and our optimized APB-free GaAs on Ge nucleation recipe.

SIMS scans showed reduced Ge contamination in the GaAs device layers for the four steps mentioned above. The largest reduction came with a combination of all four techniques which then became the growth recipe used for all further GaAs growths on Ge/GeSi/Si substrates. The final recipe for controlling Ge autodoping in GaAs was to grow a thin (200nm) GaAs cap layer on the Ge/GeSi/Si substrate, remove the substrate, polish the backside mechanically to remove about 10 μm of the wafer and all Ge at this interface, then reinsert the capped and polished substrate into a cleaned reactor tube with a new graphite susceptor. Although this procedure is complicated, it reduced the Ge autodoping in the GaAs/AlGaAs device layers to undetectable limits ($< 10^{16}$ cm^{-3}) and yielded high-quality films above the regrowth interface. The SIMS data showing this reduced Ge concentration is shown in Figure 2b.

GaAs/AlGaAs quantum-well GRINSCH laser structures were then grown on Ge/GeSi/Si substrates and tested. These devices operated cw at room temperature, demonstrating a threshold current density of 1550 A/cm^2 and a differential quantum efficiency of 0.16 at a wavelength of 858 nm. Identical devices grown on GaAs substrates showed a threshold current density of 1700A/cm^2 and a differential quantum efficiency of 0.14. The light vs. current and current vs. voltage data for the devices on Ge/GeSi/Si and GaAs are shown in Figure 3. The temperature sensitivity of both devices was also measured; the laser on Ge/GeSi/Si had a characteristic temperature T_o of 61 K, while the device on GaAs had a measured T_o of 128 K. The current-

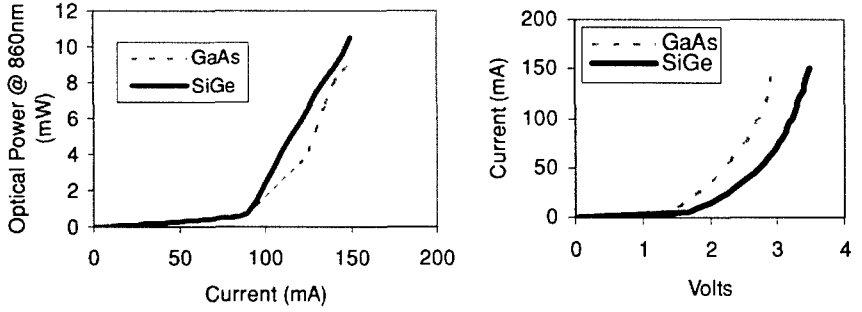

Figure 3: Side-by-side light vs. current (a.) and current vs. voltage (b.) characteristics for identical GaAs/AlGaAs GRINSCH-QW lasers grown on Ge/GeSi/Si and GaAs substrates

voltage characteristics of the device on Ge/GeSi/Si showed higher turn-on voltages and slightly larger series resistance at high current levels than the device on GaAs.

Reliability measurements were made at constant currents for both devices. The lasers on Ge/GeSi/Si showed gradual degradation after only a few minutes, and fell below threshold after a little more than 20 minutes. The device on GaAs showed no obvious degradation. A plot of the measured light intensity vs. time for two sample devices is shown in Figure 4.

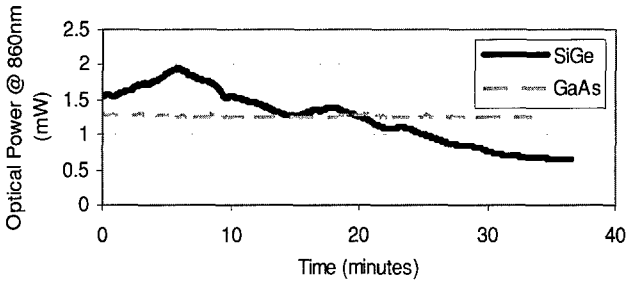

Figure 4: Lifetime measurements at constant current for representative devices on Ge/GeSi/Si and GaAs substrates. The lasing threshold power was 1mW for both devices at 860nm

The higher series resistance and lower characteristic temperature (and thus lower lifetimes) for the laser on Ge/GeSi/Si indicates that this device will require further optimization. Adding $In_xGa_{(1-x)}As$ to the active region would increase reliability by inhibiting dark-line defect propagation, if indeed that is the responsible degradation mechanism. Care would need to be taken to avoid the thermal expansion mismatch problems encountered previously, perhaps by finding a way to relax compressive strain at the growth temperature below the quantum well interface. Improved contact geometries (to avoid contacting through the double junction at the GaAs/Ge interface) and facet coating may also be useful in reducing turn-on and threshold current densities. Further investigation of the failed devices on Ge/GeSi/Si will help to understand the exact mechanisms responsible for the observed gradual degradation behaviors.

CONCLUSIONS

AlGaAs/GaAs quantum-well lasers have been demonstrated on relaxed Ge/GeSi on Si substrates for the first time. These devices operated cw at room temperature with roughly equivalent operating characteristics to identical devices grown on commercial GaAs substrates. By avoiding super-critical InGaAs quantum wells and taking steps to avoid autodoping effects from the Ge buffer layer, these lasers showed dramatic improvement over earlier devices. Device lifetimes on Ge/GeSi/Si substrates were less than 20 min at room temperature due to a still undetermined failure mechanism. Despite this rapid degradation, measured near-bulk minority carrier lifetimes in GaAs on Ge/GeSi/Si reassure us that no fundamental materials issues stand between these devices and reliable GaAs/AlGaAs/InGaAs laser operation on Si substrates. Further optimization will seek to increase device lifetimes while improving laser performance.

ACKNOWLEDGEMENTS

The authors acknowledge the financial support of the MARCO Focused Research Center on Interconnects, which is funded at MIT through a subcontract from the Georgia Institute of Technology. This work made use of the MRSEC Shared Facilities supported by the National Science Foundation under Award DMR-9400334. Additional funding was supplied by ARO Contract No. DAAG55-97-1-0111.

REFERENCES

1 H. Kroemer, Liu, T.Y., and Petroff, M., Journal of Crystal Growth **95**, 96 (1989).

2 Z. Hatzopoulos, Cengher, D., Deligeorgis, G., Androulidaki, M., Aperathitis, E., Halkias, G., Georgakilas, A., Journal of Crystal Growth **227-228**, 193 (2001).

3 Z.I. Kazi, Thilakan, P., Egawa, T., Umeno, M., and Jimbo, T., Japanese Journal of Applied Physics **40** (8), 4903 (2001).

4 P.J. Taylor, Jesser, W.A., Benson, J.D., Martinka, M., Dinan, J.H., Bradshaw, J., Lara-Taysing, M., Leavitt, R.P., Simonis, G., Chang, W., Clark, W.W., and Bertness, K.A., Journal of Applied Physics **89** (8), 4365 (2001).

5 M. T. Currie, Samavedam, S. B., Langdo, T. A., Leitz, C. W., and Fitzgerald, E. A., Applied Physics Letters **72** (14), 1718 (1998).

6 S. Ting, Bulsara, M., Yang, V., Groenert, M., Samavedam, S., Currie, M., Langdo, T., Fitzgerald, E., Joshi, A., Brown, R., Wang, X., Sieg, R., Ringel, S., presented at the SPIE Conference on Optoelectronics, San Jose, CA, 1999 (unpublished).

7 S.A. Ringel, Carlin, J.A., Leitz, C.W., Currie, M., Langdo, T., Fitzgerald, E.A., Bulsara, M., Wilt, D.M., and Clark, E.V., presented at the 16th European Photovoltaics Solar Energy Conference and Exhibition, Glasgow, Scotland, 2000 (unpublished).

8 G.R. Srinivasan, Journal of the Electrochemical Society **127** (6), 1334 (1980).

9 J.O. Carlsson, Boman, M., presented at the 9th International Conference on Chemical Vapor Deposition, Cincinnati, OH, 1984 (unpublished).

10 H. Kasano, Solid State Electronics **16**, 913 (1973).

11 S. H. Yellen, Shepard, A.H., Dalby, R.J., Baumann, J.A., Serreze, H.B., Guido, T.S., Soltz, R., Bystrom, K.J., Harding, C.M., and Waters, R.G., IEEE Journal of Quantum Electronics **29** (6), 2058 (1993).